Düzce University
Journal of Science & Technology

Research Article

Effects of Mn-site doping on the magnetocaloric properties of $La_{0.62}Bi_{0.05}Ca_{0.33}Mn_{1-x}Ru_xO_3$ manganite system

Selda KILIÇ ÇETİN [a,*], Gönül AKÇA [a], Ahmet EKİCİBİL [a]

[a] *Department of Physics, Faculty of Sciences and Letters, Çukurova University, Adana, TÜRKİYE*
** Corresponding author's e-mail address: kilics@cu.edu.tr*
doi: 10.29130/dubited.947801

ABSTRACT

This study reports the effects of Ru element doping in $La_{0.62}Bi_{0.05}Ca_{0.33}Mn_{1-x}Ru_xO_3$ (x=0.0, 0.1 and 0.2) manganite compounds on the magnetocaloric (MC) properties of materials obtained by solid-state method. XRD analysis showed that the samples crystallized in orthorhombic structure (with *Pnma* space group). The magnetic phase transition temperatures of the samples were determined from the thermomagnetic curves as 221 K for x = 0.0 sample and 215 and 206 K for x = 0.1 and x = 0.2 samples, respectively, under 100 Oe applied field. Arrott plots confirm that the type of magnetic phase transition is second-order phase transition. The $-\Delta S_M^{max}$ values were calculated as 7.55, 3.51 and 2.69 J/kgK for x = 0.0, 0.1 and 0.2 samples, respectively. Relative cooling power (RCP) values decrease with Ru doping. It was concluded that the Ru additive had an effect on reducing the transition temperatures and magnetic entropy change values of the samples.

Anahtar Kelimeler: *Magnetic entropy change, magnetocaloric effect, magnetic refrigeration, perovskites.*

Mn-bölgesi Katkılamanın $La_{0.62}Bi_{0.05}Ca_{0.33}Mn_{1-x}Ru_xO_3$ Manganit Sisteminin Manyetokalorik Özellikleri Üzerine Etkileri

ÖZ

Bu çalışma katıhal reaksiyon yöntemiyle elde edilen $La_{0.62}Bi_{0.05}Ca_{0.33}Mn_{1-x}Ru_xO_3$ (x=0.0, 0.1 ve 0.2) manganit bileşiklerinde Ru elementi katkısının malzemelerin manyetokalorik özellikleri (MC) üzerindeki etkilerini bildirmektedir. XRD analizi, numunelerin ortorombik (Pnma uzay grubu) yapıda kristalleştiğini göstermiştir. Örneklerin manyetik faz geçiş sıcaklıkları 100 Oe uygulanan alan altında katkısız x = 0.0 örneği için 221K, x = 0.1 ve x = 0.2 örnekleri için sırasıyla 215 ve 207K olarak belirlenmiştir. Arrott eğrileri tüm örneklerin ikinci dereceden faz geçişi sergilediğini doğrulamaktadır. 5 T alan altında $-\Delta S_M^{max}$ değerleri x = 0.0, 0.1 ve 0.2 örnekleri için sırasıyla 7.55, 3.51 ve 2.69 J/kgK olarak hesaplanmıştır. Örneklerin göreli soğutma güç (RCP) değerlerinde bir azalma gözlemlenmiştir. Ru katkısının örneklerin geçiş sıcaklık ve manyetik entropi değişim değerlerinde bir düşüş gösterdiği sonucuna ulaşılmıştır.

Keywords: *Manyetik entropi değişimi, manyetokalorik etki, manyetik soğutma, perovskitler.*

Received: 06/06/2021, Revised: 24/01/2022, Accepted: 28/01/2022

I. INTRODUCTION

Since conventional cooling systems used in all areas of our lives have reached limit values in terms of energy efficiency and the demand for energy has increased in all areas, there is a need to develop new technologies that can replace these systems [1]. At this point, magnetic refrigeration (MR) systems are considered to be a good alternative to conventional cooling systems [2]. The MR systems are environmentally friendly and highly energy-efficient systems compared to commonly used systems [3]. These systems work based on magnetocaloric effect (MCE) principle. The MCE is simply expressed as the observed change in temperature of the magnetic material under an external magnetic field [2], [3]. Studies on materials with magnetocaloric (MC) properties, which form the basis of innovative and environmentally friendly magnetic cooling systems, have gradually increased. In addition, the generation of electrical energy from MC materials has gained importance in recent years [4], [5] and it is predicted that these MC devices will have higher energy efficiency when compared to Peltier and Seebeck type devices [6]. In these systems, when a changing magnetic field is applied to the magnetic material surrounded by a coil, it causes an electric current to be induced in the coil during heating and cooling conditions on the material. These enable the conversion of thermal energy to electrical energy without intermediate mechanical work conversion [6]. In this sense, it is important to find materials with high MC properties both for use in MR systems and for generating electrical energy in thermomagnetic generators.

Magnetic entropy change ($-\Delta S_M$) and adiabatic temperature change (ΔT_{ad}) values are two characteristic quantities that define MCE [2]. The MC properties of many material groups have been investigated due to the fact that the main purpose of the studies on magnetic cooling is to find magnetocaloric materials with suitable criteria. [1], [7]-[9]. Although different material groups with high MC properties have been discovered, most of them cannot be used in applications due to various reasons such as the type of magnetic phase transition, thermal and magnetic hysteresis, high raw material cost and complex material production method [8].

$R_{1-x}A_xMnO_3$ (where R is rare earth elements and A: alkaline earth elements or alkaline earth metals) perovskite manganites are predicted as materials with potential to be used as cooling materials in MR applications [9]. The perovskite manganites provide many of the general criteria required for applications. For example, they have the appropriate Curie temperature; show a large MCE over a wide temperature range and their hysteresis (thermal and magnetic) are almost zero [10]. Apart from the physical properties, production, cost and production processes affect the use of materials in applications. Perovskite manganites are low cost, easy to synthesize and show good corrosion resistance properties [11]. Perovskite manganites have been extensively studied for their outstanding properties as the best cooling material for MR systems. Among the studied perovskite manganites, significant MCE was observed in $La_{0.67}Ca_{0.33}MnO_3$ perovskite manganite sample in the literature [8], [12], [13]. The effects of the variation of the average ionic radius of the A and B-sites and the material production method on the magnetocaloric properties of $La_{0.67}Ca_{0.33}MnO_3$ manganite have been studied by different research groups [14]-[17]. In the light of the literature, Gencer *et al*. examined the effect of Bi doping on the magnetic and MC properties of $La_{0.67}Ca_{0.33}MnO_3$ manganite and reported a large magnetic entropy change ($-\Delta S_M$) value for $La_{0.62}Bi_{0.05}Ca_{0.33}MnO_3$ [18]. Recently, Rutenium has been an attractive doping element among research groups to observe the effect of ionic radius variation in the B-site on the magnetic and magnetocaloric properties of manganites [19]-[22]. Different effects of Ru doping on magnetic and magnetocaloric properties have been reported [20]-[22]. With this motivation, we investigated the effect of Ru doping on the MC properties of the $La_{0.62}Bi_{0.05}Ca_{0.33}Mn_{1-x}Ru_xO_3$ (x = 0.0, 0.1 and 0.2) manganite system.

II. MATERIAL AND METHODS

Solid state reaction method was used for preparation of $La_{0.62}Bi_{0.05}Ca_{0.33}Mn_{1-x}Ru_xO_3$ (x = 0.0, 0.1 and 0.2) samples. La_2O_3, Bi_2O_3, CaO, RuO_2 and MnO_2 raw materials were used to obtain the samples.

Sigma-Aldrich brand was preferred in the selection of raw materials of suitable purity. The raw materials determined according to stoichiometric ratio were mixed and ground for 60 minutes. Then, the solid solution was calcined in air at 600 ˚C for 6 h. Then the grinding process was repeated. The samples were pressed into tablets and sintered at 1200 ˚C for 24 h in air. The $La_{0.62}Bi_{0.05}Ca_{0.33}Mn_{1-x}Ru_xO_3$ (x = 0.0, 0.1 and 0.2) samples were denominated in the study as LBCM for x = 0.0, LBCMR-1 for x = 0.1 and LBCMR-2 for x = 0.2. The structural, magnetic and MC properties of the samples and the effect of Ru doping on these properties were investigated in detail. X-ray diffractometer (XRD) and Scanning Electron Microscope (SEM) were used for structural analyses. XRD measurements were performed over the range of $10^o \leq 2\theta \leq 80^o$ in increments of 0.0131º. Magnetization measurements ($M(T)$ and $M(H)$) were obtained by using PPMS (Physical Property Measurement System, DynaCool-9) to determine magnetic properties and calculate magnetic entropy change values ($-\Delta S_M$).

III. RESULTS AND DISCUSSION

The x-ray diffraction pattern of the LBCM is shown in Fig.1a. The observed and calculated x-ray pattern of the LBCM sample is represented by the red and black lines, respectively. The difference between the observed and the calculated is plotted by the blue line. Bragg reflections are indicated by green ticks. The XRD patterns of LBCM, LBCMR-1 and LBCMR-2 samples are given in Fig.1b. It is seen that the diffraction peaks, which are compatible with the perovskite structure, are sharp and narrow. High Score Plus software was used to define phases and crystal structure. The diffraction peaks for all samples matched the orthorhombic system with *Pnma* space group. In addition, small peaks belonging to the Mn_3O_4 phase (marked with Δ in Fig.1) are observed in the diffraction patterns of the samples. The Bragg position and miller indices of the samples are seen in Fig. 1b. The lattice parameters (a, b and c cell parameters) and unit cell volume (V) of the samples were determined by FullProf program. The results obtained for the samples are given in Table 1. It is seen that Ru doping to the Mn-site causes an increase in a, b and c cell parameters and V values. Since the radius of the Ru^{4+} ion is higher than that of the Mn^{4+} ion [23], an increase in the mean ionic radius ($<r_{Mn}>$) of the Mn-region was observed. This induces the changing of the a, b and c cell parameters. As a result, the V values of the samples change. The perovskite structure is preserved when the tolerance factor is between 0.75 and 1 [24]. This factor is given by the following equation,

$$t = (r_A + r_O)/\sqrt{2}(r_{Mn} + r_O) \quad (1)$$

where the ionic radii of the A cation, Mn cation and oxygen are represented with r_A, r_{Mn} and r_O, respectively. The t value is a measure of whether the structure can remain stable after doping in the A and B regions, and is used to determine the mismatch between the A-O and Mn-O bond lengths. The calculated t values of the samples are given in Table 1. The variation of the results between 0.75 and 1 confirms that the samples show perovskite structure. It was observed that the t values of the samples decreased with the increase of Ru doping. The decrease in t is due to Ru (0.705 Å) having a higher ionic radius than Mn (0.645 Å) [23]. Addition of the higher ionic radius element to the Mn-site causes $<r_{Mn}>$ to increase and t to decrease. However, the change in t value for samples does not affect the crystal structure.

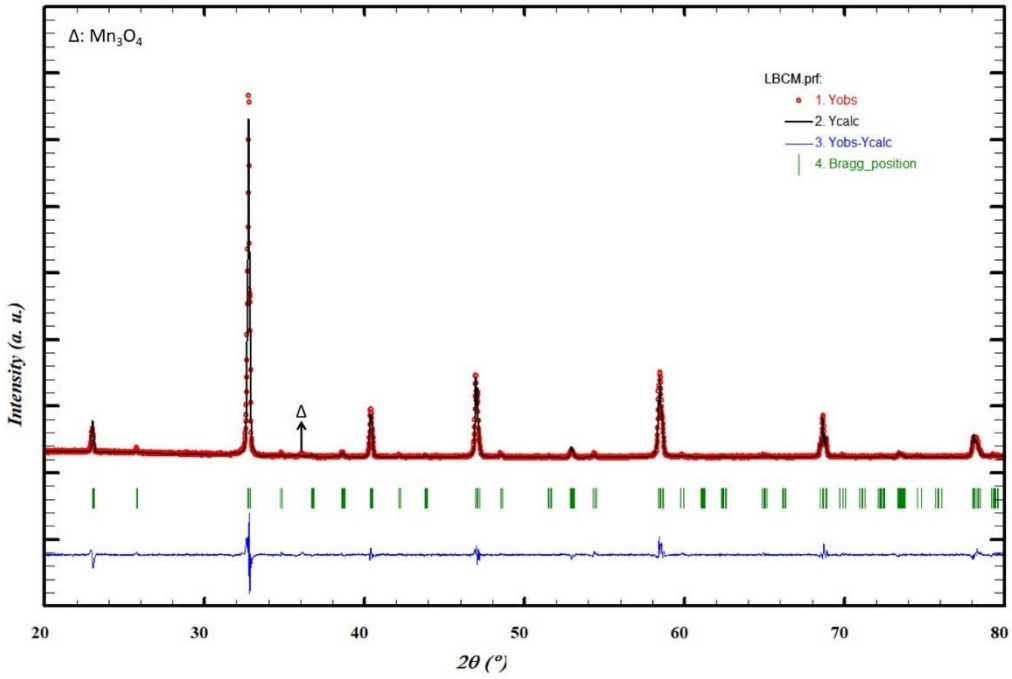

(a)

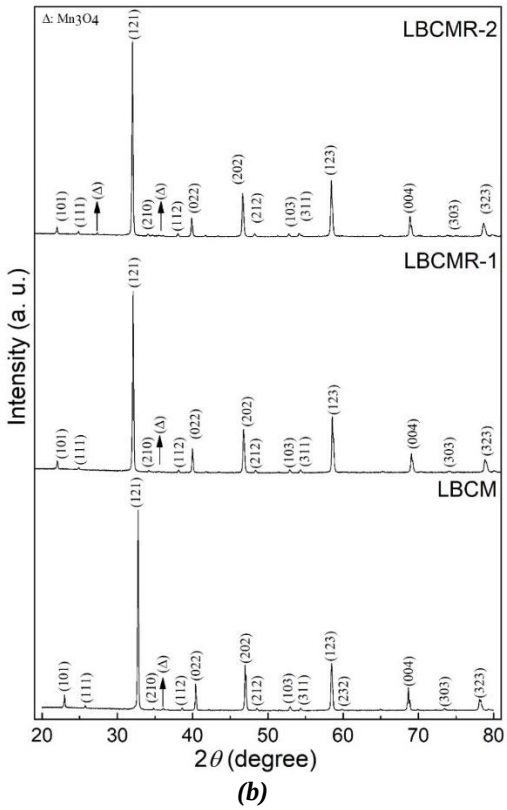

(b)

Figure 1. (a) *Rietveld plot of the LBCM sample.* ***(b)*** *X-ray diffraction patterns for LBCM, LBCMR-1 and LBCMR-2 samples.*

Tablo 1. *Some structural parameters of the* $La_{0.62}Bi_{0.05}Ca_{0.33}Mn_{1-x}Ru_xO_3$ *manganites.*

Sample	***a*** **(Å)**	***b*** **(Å)**	***c*** **(Å)**	***V*** **(Å^3)**	***t***
LBCM	5.4647	7.7294	5.4837	231.6273	0.9481
LBCMR-1	5.4768	7.7434	5.4921	232.9128	0.9427
LBCMR-2	5.4921	7.7666	5.5010	234.6443	0.9373

The morphology and composition of the samples are generally investigated by SEM/EDS measurements, which is a convenient and sufficient method [25]. We obtained SEM images and EDS spectra of the samples given in Figure 2a-c in order to investigate the morphological properties and elemental composition. It is seen that the EDS spectra of the samples contain peaks belonging to La, Bi, Ca, Mn and O atoms. In addition, the fact that no peak belonging to any other element was observed in the EDS spectra indicates that there is no impurity peak belonging to the sample production process and that no elemental loss has been experienced in this process. From the SEM images of the samples, it is seen that the volumetric particle structures have different sizes and in different polygonal shapes. For all samples, it is seen that there are intergranular gaps. The volume of these gaps increases with increasing Ru doping. This means that the intergranular connectivity is adversely affected. Besides, it is seen that the grain boundaries that are evident for LBCM samples become indistinct with increasing Ru contribution. This means that the Ru doping may adversely affect the physical properties of the samples. By using Image J Software, the size distribution histogram for the LCBM sample is given Fig.2d. The average grain size of the particles is 2.03, 3.75 and 2.52 μm for LBCM, LBCMR-1 and LBCMR-2 samples, respectively.

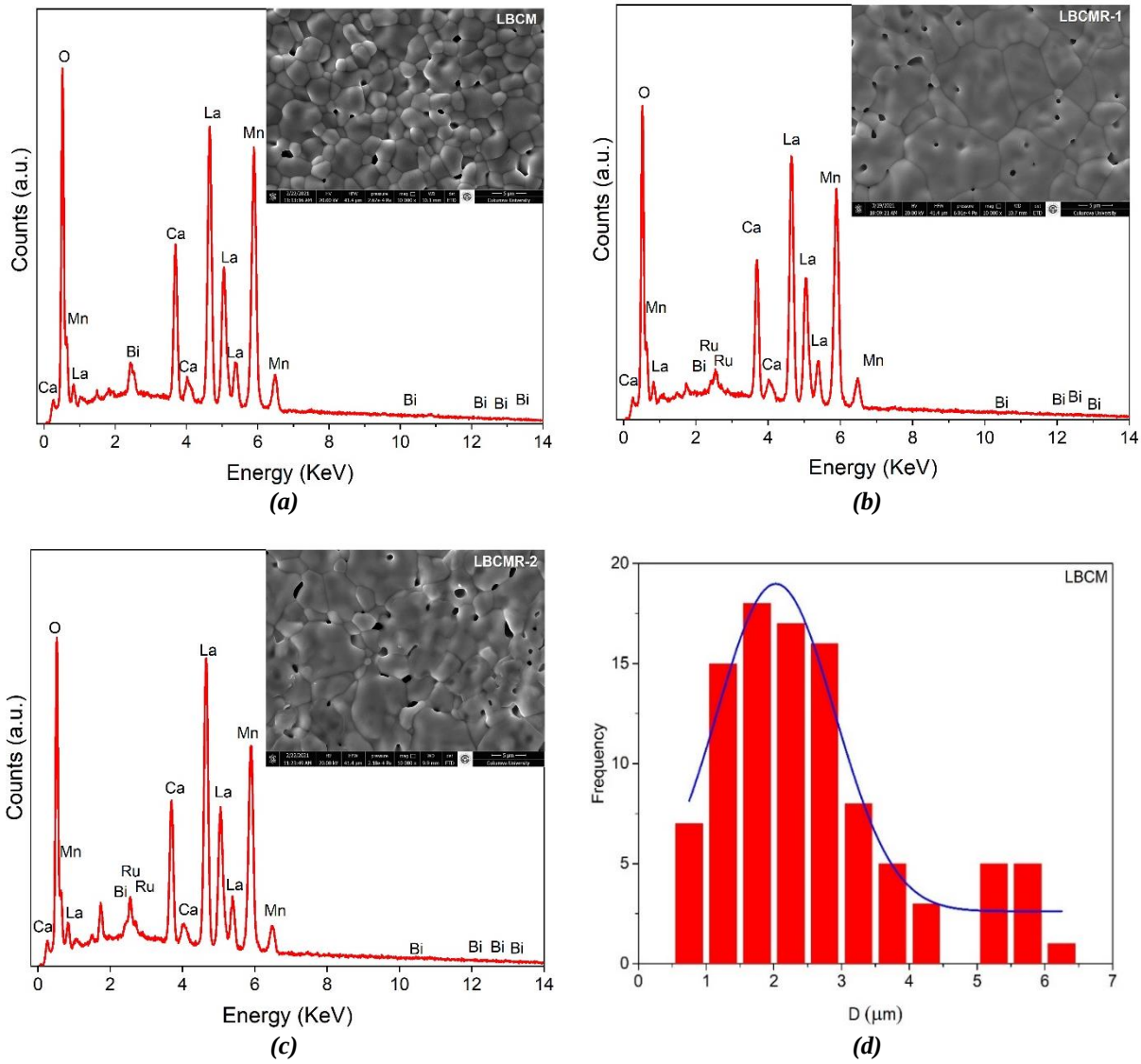

Figure 2.(a-c) *The EDS spectra and SEM images taken at 10 KX magnification of the samples,* ***(d)*** *The size distribution histogram for LBCM sample.*

To investigate the magnetic structure of the samples and their magnetic properties, we have performed the *M*(*T*) measurements for all samples in ZFC and FC modes. In both modes, 100 Oe magnetic field

was applied to the samples. Figure 3a-c show the $M(T)$ curves. Both $M(T)_{ZFC}$ and $M(T)_{FC}$ curves of the samples show similar behavior with temperature. That is, with increasing temperature, the magnetization decreases and its value drops to almost zero at a certain temperature, meaning that the samples show a phase transition from ferromagnetic (FM) to paramagnetic (PM). For the LBCM sample, this transition occurs in a narrower temperature range than for the LBCMR-1 and LBCMR-2 samples. This situation points out that the magnetic entropy change value ($-\Delta S_M$) of the LBCM sample may be higher than that of the other samples. From the $M(T)$ curves of all samples, at the low-temperature region, it is seen that the ZFC and FC magnetization values show a difference that may arise from magnetic anisotropy, domain wall pinning effect and canted nature of spin [26]. The observed difference between magnetization values shows an increase with increasing Ru doping. The magnetic phase transition temperature called as Curie temperature (T_C) is generally determined from the inflection point of the dM/dT (T) curve. T_C values of the LBCM, LBCMR-1 and LBCMR-2 samples are 221, 215 and 207 K, respectively. Gencer *et al*. [27] have been reported that the T_C value of the LBCM sample is 248 K. It is seen that there is a difference that may arise from processes of material production [27], [28]. The T_C value of the perovskite manganite strongly depends on the Mn^{3+}/Mn^{4+} ratio [29], [30]. The change in this ratio affects the physical properties of the manganite and this is explained by double exchange interaction [31], [32]. With Ru doping in the Mn-site, the ratio of Mn^{3+}/Mn^{4+} changes, resulting in a decrease in T_C.

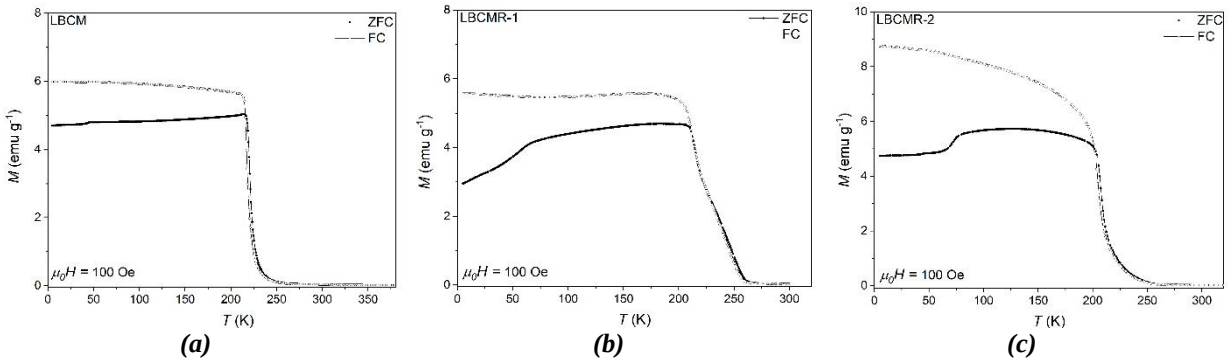

Figure 3. (a-c) *The M(T) curves of the samples at ZFC and FC modes.*

Fig. 4a-c show isothermal magnetization curves for the LBCM, LBCMR-1 and LBCMR-2 samples performed under applied magnetic fields up to 5 T around T_C values of the samples. Above the T_C, the *M(H)* curves of the samples change linearly with increasing magnetic field. This behavior verifies that all samples exhibit PM property. At low temperatures, the $M(H)$ curves of the LBCM, LBCMR-1 and LBCMR-2 samples change rapidly with increasing magnetic field and reach saturation. The samples show FM properties. For the LBCM sample only, the $M(H)$ curves show a rapid increase of magnetization like a sharp step at a threshold field known as metamagnetic transition. The metamagnetic transition implies that the FM and AFM-CO phases may coexist [33].

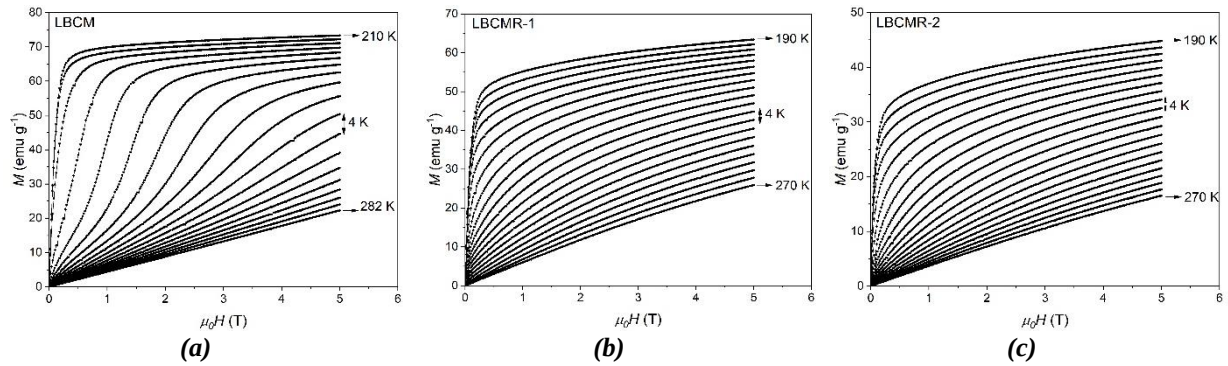

Figure 4. (a-c) *The M(H) curves of the samples.*

The type of the magnetic phase transition for MC materials is a quite important parameter that affects the usability of that material in MR technology applications. This parameter is related to direct the working efficiency and the reversibility of a magnetic refrigerant [8]. The samples show first order magnetic phase transition (FOMT) or second order phase transition (SOMT). If the samples exhibit FOMT, their magnetic and thermal hysteresis is large which negatively affects the working efficiency and reversibility of the system. According to the explanations mentioned above, in the way of the practical applications, both the hysteresis of the samples should be as small as possible [8]. A Banerjee criterion is mostly used to determine the order of the magnetic phase transition [34]. According to this criterion, the Arrott plots ($\mu_0 H/M$ versus M^2 curves) of the samples are obtained from the $M(H)$ measurements. If the Arrott plots have a positive slope around T_C, the phase transition of the samples is the SOMT. Otherwise, the transition is first order. The Arrott plots of the samples are given in Fig.5a-c. These curves for all samples have positive slope around T_C. According to this result, the samples show SOMT.

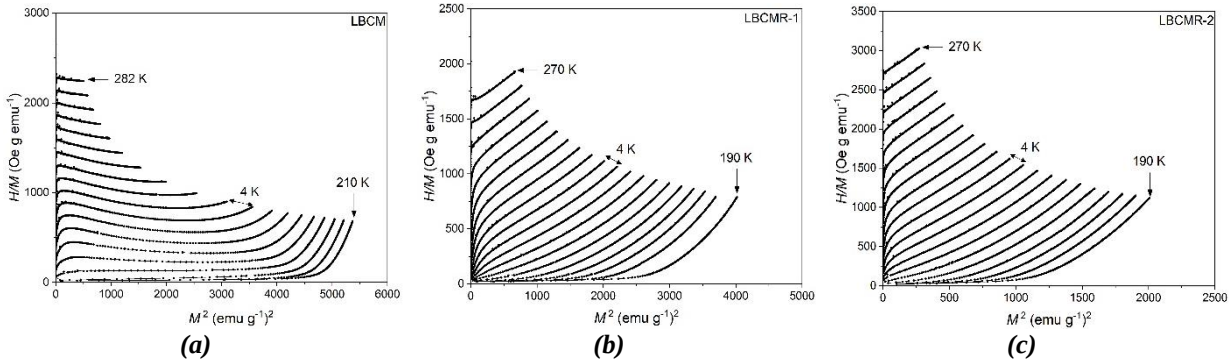

Figure 5. (a-c) *The Arrott plots of the samples.*

The $-\Delta S_M$ and ΔT_{ad} are the two fundamental quantities describing MCE [2, 8]. These quantities can be determined by direct or indirect measurement methods. While ΔT_{ad} is measured by direct measurement methods, the numeric value of $-\Delta S_M$ is calculated indirectly with the following equation [2].

$$-\Delta S_M(H,T) = \sum \frac{M_i - M_{i+1}}{T_{i+1} - T_i} \Delta H_i. \qquad (2)$$

In the equation, M and T represent magnetization and temperature, respectively. We have calculated -ΔS_M values of the samples under different magnetic fields and obtained the curves of -ΔS_M as a function of the temperature. The -ΔS_M curves of the samples are given in Figs. 6a-c. The curves around T_C show a maximum peak defined as the maximum magnetic entropy change ($-\Delta S_M^{max}$). The $-\Delta S_M^{max}$ value is 5.99, 1.86 and 1.41 J/kgK under 2 T magnetic fields for LBCM, LBCMR-1 and LBCMR-2, respectively. It is seen that there is a decrease in this value with the contribution of Ru. This result may arise from the change observed in Mn^{3+}/ Mn^{4+} ratio and grain sizes of the samples.
The RCP is one of the criteria that is as important as the $-\Delta S_M$ and ΔT_{ad} values in the selection of the MC materials for MR applications [2], [8], [10]. The total cooling energy of the MC material given as (J/kg) by RCP [35]. The RCP term formulizes with the product of $-\Delta S_M^{max}$ by δT_{FWHM}, where δT_{FWHM} is the full width at half maximum of the -ΔS_M (T) curves. RCP values at 2 T for LBCM, LBCMR-1 and LBCMR-2 samples were calculated as 107.82, 81.84 and 43.71 J/kg, respectively. With Ru doping at Mn-site, it is observed the RCP values decrease. According to obtained results, the replacement of Ru with Mn caused a decrement in values of magnetic entropy change and RCP. The decrease in the values of $-\Delta S_M^{max}$ and RCP is compatible with Ru-doped studies in the literature [19], [21].

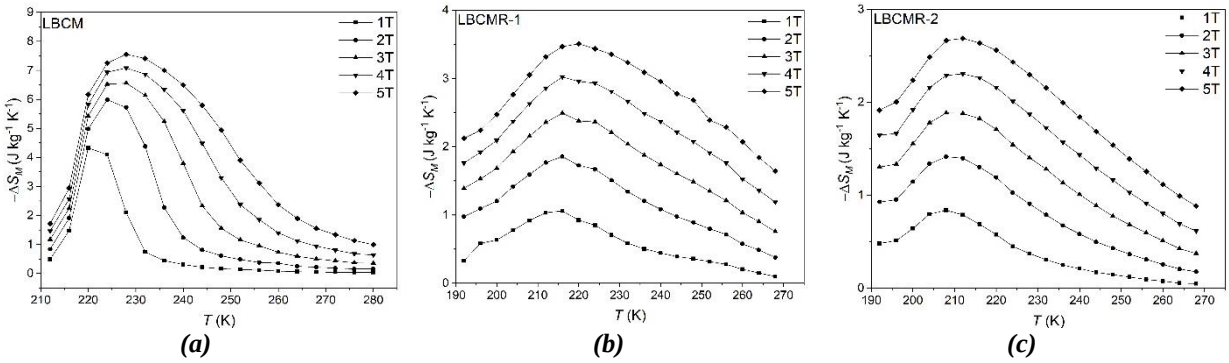

Figure 6. (a-c) *-ΔS_M (T) curves of the samples for different magnetic fields*

IV. CONCLUSION

In this study, we have investigated the magnetocaloric properties of $La_{0.62}Bi_{0.05}Ca_{0.33}Mn_{1-x}Ru_xO_3$ (x=0.0, 0.1 and 0.2) samples. All samples were prepared by solid state method. The samples analyzed by XRD technique at room temperature crystallize in orthorhombic structure. From $M(T)$ measurements, it is understood that all samples exhibited a magnetic phase transition from FM to PM. T_C values of the LBCM, LBCMR-1 and LBCMR-2 samples are determined as 221, 215 and 207 K, respectively. The T_C value of the samples decreases with increasing Ru concentration. The decrease in T_C may arise from the changing of the Mn^{3+}/Mn^{4+} ratio with Ru doping. It is also thought that this decrease is due to presence of Ru^{4+}-O-Ru^{4+} super exchange interactions in the structure, weakening the double exchange interactions. From the Arrott plots, it can be seen that all samples show the SOMT. The $-\Delta S_M^{max}$ value is 5.99, 1.86 and 1.41 J/kgK under 2 T magnetic fields for LBCM, LBCMR-1 and LBCMR-2, respectively. The RCP values under 2 T for LBCM, LBCMR-1 and LBCMR-2 samples were found to be 107.82, 81.84 and 43.71 J/kg, respectively. The results showed that with the increase of Ru addition, the double exchange interactions and accordingly, the transition temperature and MC properties were negatively affected. Besides, a large $-\Delta S_M^{max}$ and RCP values were obtained for the LBCM sample, and in this sense, this material can be considered as a candidate cooling material for magnetic cooling applications in the 200-250 K temperature range.

ACKNOWLEDGMENTS: This work is supported by the Research Fund of Çukurova University, Adana, Turkey, under grant contracts no: FBA-2019-12320.

V. REFERENCES

[1] V. Franco, J. S. Blázquez, J. J. Ipus, J. Y. Law, L. M. Moreno-Ramírez, A. Conde, "Magnetocaloric effect: from materials research to refrigeration devices," *Prog. Mater. Sci.*, vol. 93, pp. 12-232, 2018.

[2] A. M. Tishin, Y. I. Spichkin, *The Magnetocaloric Effect and its Applications*, 1st ed., London, UK: IOP Publishing LTD, 2003, ch. 11, pp. 351-401.

[3] V. K. Pecharsky, K. A. Gschneidner Jr., "Advanced magnetocaloric materials: what does the future hold?," *Int. J. Refrig.*, vol. 29, pp. 1239–1249, 2006.

[4] R. A. Kishore, S. Priya, "A review on design and performance of thermomagnetic devices," *Renew. Sust. Energ. Rev.*, vol. 81, pp. 31-44, 2018.

[5] A. Waske, D. Dzekan, K. Sellschopp, D. Berger, A. Stork, K. Nielsch, S. Faehler, "Energy harvesting near room temperature using a thermomagnetic generator with a pretzel-like manetic flux topology," *Nat. Energy*, vol. 4, pp. 68-74, 2019.

[6] E. Brück, "Thermomagnetic generator," *Patent Application Pub.* 0037342, Apr. 28, 2011.

[7] E. Brück, "Developments in magnetocaloric refrigeration," *J. Phys. D: Appl. Phys.*, vol. 38, pp. R381–R391, 2005.

[8] M. H. Phan, S. C. Yu, "Review of the magnetocaloric effect in manganite materials," *J. Magn. Magn. Mater*., vol. 308, pp. 325–340, 2007.

[9] Y. Xu, M. Meier, P. Das, M. R. Koblischka, U. Hartmann, "Perovskite manganites: potential materials for magnetic cooling at or near room temperature," *Cryst. Eng*., vol. 5, pp. 383-389, 2002.

[10] B. F. Yu, Q. Gao, B. Zhang, X. Z. Meng, Z. Chen, "Review on research of room temperature magnetic refrigeration," *Int. J. Refrig.*, vol. 26, pp. 622-636, 2003.

[11] A. Kitanovski, J. Tušek, U. Tomc, U. Plaznik, M. Ožbolt, A. Poredoš, "Magnetocaloric materials for freezing, cooling, and heat-pump applications," in *Magnetocaloric Energy Conversion*, 1st ed., Cham, Switzerland: Springer, 2015, ch. 2, pp. 23-37.

[12] Z. B. Guo, Y. W. Du, J. S. Zhu, H. Huang, W. P. Ding, D. Feng, "Large Magnetic Entropy Change in Perovskite-Type Manganese Oxides," *Phys. Rev. Lett*., vol. 78, pp. 1142-1145, 1997.

[13] G. C. Lin, Q. Wei, J. X. Zhang, "Direct measurement of the magnetocaloric effect in $La_{0.67}Ca_{0.33}MnO_3$," *J. Magn. Magn. Mater*., vol. 300, pp. 392-396, 2006.

[14] X. X. Zhang, J. Tejada, Y. Xin, G. F. Sun, K. W. Wong, X. Bohigas, "Magnetocaloric effect in $La_{0.67}Ca_{0.33}MnO$ and $La_{0.60}Y_{0.07}Ca_{0.33}MnO$ bulk materials," *Appl. Phys.*, vol. 63, no. 23, pp. 3596-3598, 1996.

[15] V. S. Kolat, H. Gencer, M. Gunes, S. Atalay, "Effect of B-doping on the structural, magnetotransport and magnetocaloric properties of $La_{0.67}Ca_{0.33}MnO_3$ compounds," *Mater. Sci. Eng. B*, vol. 140, pp. 212-217, 2007.

[16] P. Nisha, S. S. Pillai, M. R. Varma, K. G. Suresh, "Influence of cobalt on the structural, magnetic and magnetocaloric properties of $La_{0.67}Ca_{0.33}MnO_3$," *J. Magn. Magn. Mater*., vol. 327, pp. 189-195, 2013.

[17] Y. Regaieg, F. Ayadi, J. Monnier, S. Reguer, M. Koubaa, A. Cheikhrouhou, S. Nowak, L. Sicard, S. Ammar-Merah, "Magnetocaloric properties of $La_{0.67}Ca_{0.33}MnO_3$ produced by reactive spark plasma sintering and by conventional ceramic route," *Mater. Res. Express*, vol. 1, 046105, 2014.

[18] H. Gencer, S. Atalay, H. I. Adıguzel, V. S. Kolat, "Magnetocaloric effect in the $La_{0.62}Bi_{0.05}Ca_{0.33}MnO_3$ compound," *Physica B*, vol. 357, pp. 326–333, 2005.

[19] A. O. Ayaş, S. Kılıç Çetin, M. Akyol, G. Akça, A. Ekicibil, "Effect of B site partial Ru substitution on structural magnetic and magnetocaloric properties in $La_{0.7}Pb_{0.3}Mn_{1-x}Ru_xO_3$ (x= 0.0, 0.1 and 0.2) perovskite system," *J. Mol. Struct.*, vol. 1200, 127120, 2020.

[20] Z. Mohamed, I. S. Shahron, N. Ibrahim , M. F. Maulud, "Influence of Ruthenium Doping on the Crystal Structure and Magnetic Properties of $Pr_{0.67}Ba_{0.33}Mn_{1-x}Ru_xO_3$ Manganites," *Crystals*, vol. 10, no. 4, 295, 2020.

[21] M. Pektas, T. Izgi, H. Gencer, S. Atalay, V. S. Kolat, N. Bayri, "Effects of Ru substitution on the structural, magnetic and magnetocaloric properties of $Pr_{0.68}Ca_{0.22}Sr_{0.1}Mn_{1-x}Ru_xO_3$ (x = 0, 0.05, 0.1 and 0.2) compounds," *J. Mater. Sci.: Mater. Electron.*, vol. 31, pp. 15731–15741, 2020.

[22] A. Bhargav, M. Prajapat, D. S. Rana, S. P. Sanyal, "Magnetic Properties of Ru-Doped $Nd_{0.67}Sr_{0.33}Mn_{1-x}Ru_xO_3$ ($0 \leq x \leq 0.10$) Manganites," *J. Supercond. Nov. Magn.*, vol. 32, pp. 1991–1996, 2019.

[23] R. D. Shannon, "Revised effective ionic radii and systematic studies of interatomic distances in halides and chalcogenides," *Acta Crystallogr. Sect.* A, vol. 32, pp. 751- 767, 1976.

[24] S. Tarhouni, A. Mleiki, I. Chaaba, H. B. Khelifa, W. Cheikhrouhou-Koubaa, M. Koubaa , A. Cheikhrouhou, E. K. Hlil, "Structural, magnetic and magnetocaloric properties of Ag-doped $Pr_{0.5}Sr_{0.5-x}Ag_xMnO_3$ manganites ($0.0 \leq x \leq 0.4$)," *Ceram. Int.*, vol. 43, pp. 133-143, 2017.

[25] M. K. Verma, N. D. Sharma, N. Choudhary, S. Sharma, D. Singh, "Comparative study of $La_{0.6}R_{0.1}Ca_{0.3}Mn_{0.9}Cr_{0.1}O_3$ (R = La, Eu and Ho) nanoparticles: effect of A-cation size and sintering temperature," *J. Mater. Sci. : Mater. Electron.*, vol. 30, pp. 12328–12338, 2019.

[26] S. Kılıç Çetin, G. Akça, A. Ekicibil, "Impact of small Er rare earth element substitution on magnetocaloric properties of $(La_{0.9}Er_{0.1})_{0.67}Pb_{0.33}MnO_3$ perovskite," *J. Mol. Struct.*, vol. 1196, pp. 658-661, 2019.

[27] F. Ayadi, S. Ammar, S. Nowak, W. Cheikhrouhou-Koubaa, Y. Regaieg, M. Koubaa, J. Monnier, L. Sicard, "Importance of the synthesis and sintering methods on the properties of manganite ceramics: The example of $La_{0.7}Ca_{0.3}MnO$," *J. Alloys Compd.*, vol. 759, pp. 52-59, 2018.

[28] M. Oumezzine, O. Peña, T. Guizouarn, R. Lebullenger, M. Oumezzine, "Impact of the sintering temperature on the structural, magnetic and electrical transport properties of doped $La_{0.67}Ba_{0.33}Mn_{0.9}Cr_{0.1}O_3$ manganite,"*J. Magn. Magn. Mater*., vol. 324, no. 18, pp. 2821-2828, 2012.

[29] A. Selmi, R. M'nassri, W. Cheikhrouhou-Koubaa, N. C. Boudjada, A. Cheikhrouhou, "The effect of Co doping on the magnetic and magnetocaloric properties of $Pr_{0.7}Ca_{0.3}Mn_{1-x}Co_xO_3$ manganites," *Ceram. Int.*, vol. 41, pp. 7723-7728, 2015.

[30] M. Dhahri, A. Zaidi, K. Cherif, J. Dhahri, E. K. Hlil, "Effect of indium substitution on structural, magnetic and manganites magnetocaloric properties of $La_{0.5}Sm_{0.1}Sr_{0.4}Mn1\text{-}xIn_xO_3$ ($0 \leq x \leq 0.1$)," *J. Alloys Compd.*, vol. 691, pp. 578-586, 2017.

[31] C. Zener,"Interaction between the d-shells in the transition metals. II. ferromagnetic compounds of manganese with perovskite structure," *Phys. Rev.*, vol. 82, pp. 403-405, 1951.

[32] R. Mahendiran, S. K. Tiwary, A. K. Raychaudhuri, T. V. Ramakrishnan, "Structure, electron-transport properties, and giant magnetoresistance of hole-doped $LaMnO_3$ systems," *Phys. Rev. B*, vol. 53, pp. 3348-3358, 1996.

[33] V. S. Kolat, T. Izgi, A. O. Kaya, N. Bayri, H. Gencer, S. Atalay, "Metamagnetic transition and magnetocaloric effect in charge-ordered $Pr_{0.68}Ca_{0.32-x}Sr_xMnO_3$ (x=0, 0.1, 0.18, 0.26 and 0.32) compounds," *J. Magn. Magnet. Mater*., vol. 32, pp. 427-433, 2010.

[34] B. K. Banerjee, "On a generalised approach to first and second order magnetic transitions," *Phys. Lett*., vol. 12, pp. 16-17, 1964.

[35] M. Botello-Zubiate, M. Grijalva-Castillo, D. Soto-Parra, R. Sáenz-Hernández, C. Santillán-Rodríguez, and J. Matutes-Aquino, "Preparation of $La_{0.7}Ca_{0.3-x}Sr_xMnO_3$ manganites by four synthesis methods and their influence on the magnetic properties and relative cooling power," *Materials*, vol. 12, no. 2, pp. 309, 2019.